Activity of the β-catenin phosphodestruction complex at cell–cell contacts is enhanced by cadherin-based adhesion

Meghan T. Maher,[1,2] Annette S. Flozak,[1] Adam M. Stocker,[2,3] Anjen Chenn,[3,4] and Cara J. Gottardi[1,4]

[1]Department of Medicine, [2]Integrated Graduate Program in the Life Sciences, [3]Department of Pathology, and [4]Robert H. Lurie Comprehensive Cancer Center, Feinberg School of Medicine, Northwestern University, Chicago, IL 60611

It is well established that cadherin protein levels impact canonical Wnt signaling through binding and sequestering β-catenin (β-cat) from T-cell factor family transcription factors. Whether changes in intercellular adhesion can affect β-cat signaling and the mechanism through which this occurs has remained unresolved. We show that axin, APC2, GSK-3β and N-terminally phosphorylated forms of β-cat can localize to cell–cell contacts in a complex that is molecularly distinct from the cadherin–catenin adhesive complex. Nonetheless, cadherins can promote the N-terminal phosphorylation of β-cat, and cell–cell adhesion increases the turnover of cytosolic β-cat. Together, these data suggest that cadherin-based cell–cell adhesion limits Wnt signals by promoting the activity of a junction-localized β-cat phosphodestruction complex, which may be relevant to tissue morphogenesis and cell fate decisions during development.

Introduction

The protein β-catenin (β-cat) serves two functions that are fundamental to tissue structure and function. As a central component of intercellular adherens junctions, β-cat links cadherin adhesion receptors to the actin cytoskeleton through the actin-binding protein α-catenin. As a key component of the Wnt signaling cascade, β-cat partners with lymphocyte enhancer factor/T-cell factor (TCF) family DNA-binding proteins to recruit chromatin-modifying factors required for gene expression (for review see Willert and Jones, 2006). The fact that cells use β-cat in both cell–cell adhesion and transcriptional activation has long suggested that these two processes may be coordinated. Indeed, gain- and loss-of-function studies support a model in which cadherins directly sequester β-cat from the nucleus and serve as a sink for the Wnt-generated cytosolic pool of β-cat (Heasman et al., 1994; Cox et al., 1996; Fagotto et al., 1996). However, whether changes in cell–cell adhesion, rather than changes in cadherin abundance, can affect Wnt signaling has remained unanswered.

In the absence of Wnt, β-cat activity is largely regulated by a multiprotein complex that mediates the phosphorylation-dependent destruction of cytosolic β-cat. Specifically, the scaffold protein axin recruits two Ser/Thr kinases, CK1-α and GSK-3β, directing an ordered phosphorylation of β-cat at Ser45 (by CK1-α) and subsequently at Thr41, Ser37, and Ser33 (by GSK-3β; Liu et al., 2002). Phosphorylated Ser33 and Ser37 are recognized by the E3 ligase β-TrCP (transducin repeat–containing protein), which leads to the ubiquitylation and degradation of β-cat (Hart et al., 1999). The tumor suppressor adenomatous polyposis coli (APC) appears to facilitate the flux of β-cat through the complex by displacing axin (Ha et al., 2004). APC2 is a second APC gene expressed in most epithelia (van Es et al., 1999). Unlike the APC mutated in colon cancers and found at the ends of microtubules, APC2 localizes to actin-rich structures (McCartney et al., 1999; Yu and Bienz, 1999; Yu et al., 1999). Although gain- and loss-of-function studies show that both APCs can inhibit β-cat signaling (McCartney et al., 1999; van Es et al., 1999; Yu et al., 1999; Polakis, 2000), the different subcellular distributions of APC and APC2, along with evidence that APC2 protein expression is maintained in

The Rockefeller University Press $30.00
J. Cell Biol. Vol. 186 No. 2   219–228
www.jcb.org/cgi/doi/10.1083/jcb.200811108

JCB   219

APC mutant tumors (Jarrett et al., 2001), suggest that they participate in different phosphodestruction complexes that are subject to distinct regulation.

Wnts are the best-known inhibitors of the β-cat phosphodestruction complex. These ligands engage a receptor complex and induce the local inactivation of GSK-3β within and/or disruption of the axin scaffold complex (Klaus and Birchmeier, 2008). As a result, an N-terminally hypophosphorylated form of β-cat accumulates, translocates to the nucleus, and activates TCF/lymphocyte enhancer factor family transcription factors. In this study, we show that N-terminal phospho forms of β-cat and components of the phosphodestruction complex are localized to sites of cell contact, where the activity of this complex can be enhanced by cadherin-based cell adhesion.

Results and discussion

Epithelial cadherin (E-cad) reduces levels of the signaling form of β-cat by promoting its N-terminal phosphorylation

The SW480 colon carcinoma cell line exhibits robust β-cat/TCF signaling because of a loss-of-function mutation in APC and low levels of E-cad. Restoration of E-cad expression reduced the oncogenic signaling activity of β-cat without markedly sequestering cytosolic β-cat (Gottardi et al., 2001). This finding raised the possibility that Wnts might generate a minor, transcriptionally active form of β-cat used for both signaling and adhesion. Alternatively, the cadherin might inhibit β-cat signaling through a mechanism that catalytically inactivates the bulk pool of β-cat.

It is now appreciated that β-cat unphosphorylated at Ser33, Ser37, and Thr41 is more transcriptionally active than forms of β-cat phosphorylated at these sites (Guger and Gumbiner, 2000; Staal et al., 2002). Several recently developed reagents allow for detection of these specific phosphorylated and unphosphorylated epitopes in the N terminus of β-cat (Fig. 1 A). Because SW480 cells are mutant for APC, the regulation and localization of these phospho forms of β-cat, which are normally coupled with ubiquitylation and degradation, can be characterized.

Using the mock (−E-cad) and E-cad–transfected cell lines previously described (Gottardi et al., 2001), we confirm that total levels of β-cat are unchanged by cadherin expression (Fig. 1 B). However, using an antibody that recognizes the signaling form of β-cat (Staal et al., 2002; van Noort et al., 2002), we observe an inverse correlation between E-cad levels and the abundance of this hypophosphorylated form of β-cat (active β-cat [ABC]; Fig. 1 B). Even mock-transfected SW480 cells, which normally express low levels of endogenous E-cad, upregulate E-cad in densely plated cultures and correlate with reduced ABC (Fig. 1 B, third lane vs. first lane). The total amount of β-cat appears unchanged, suggesting that E-cad may promote the phosphorylation of β-cat and thereby loss of the unphosphorylated epitope. To test this, we used antibodies that recognize β-cat phosphorylated on Thr41 and Ser45 (phospho-41/45 [P41/45]; Fig. 1 A) and observe an E-cad–dependent increase in β-cat phosphorylated at these sites (Fig. 1 C). As
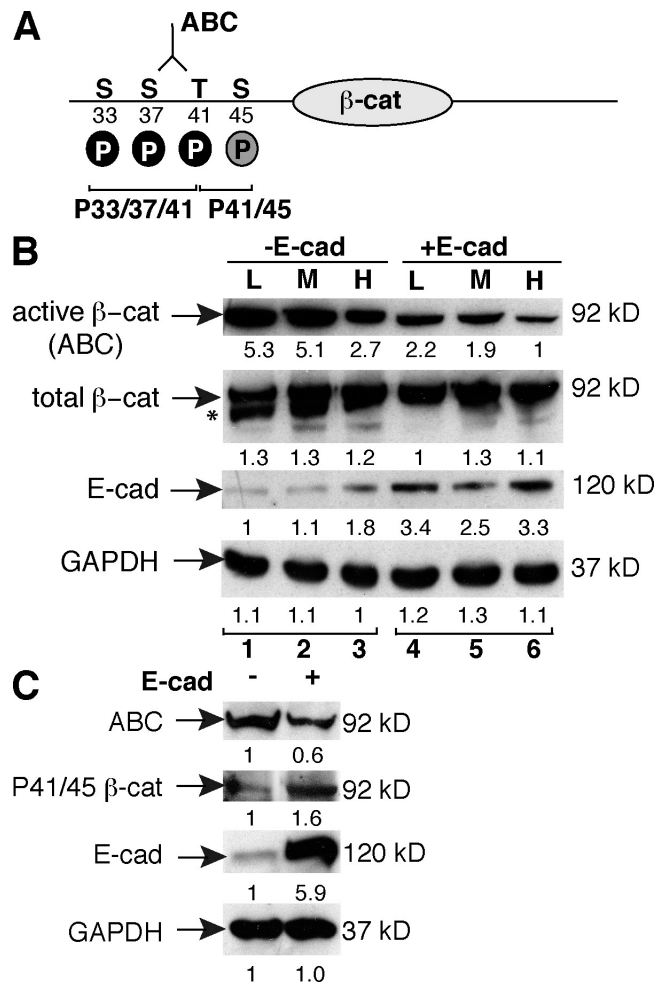

Figure 1. **Restoring E-cad expression in SW480 cells alters the phosphorylation status of the β-cat N terminus.** (A) β-cat N-terminal epitopes recognized by antibodies to ABC (unphosphorylated at Ser37 and Thr41), P33/37/41, and P41/45. The CK1-α site is gray; GSK-3β sites are black. (B) Immunoblots of SW480 control (−E-cad) or E-cad–expressing cell lysates cultured at low (L), medium (M), or high (H) density. The asterisk denotes a faster migrating, possibly hypophosphorylated form of β-cat that disappears with increasing E-cad expression. (C) The abundance of P41/45 β-cat increases with E-cad expression. (B and C) The numbers below each lane reflect normalized densitometry values.

phosphorylation at these residues is associated with reduced signaling activity (Guger and Gumbiner, 2000; Staal et al., 2002), these data suggest that E-cad may be able to inhibit β-cat signaling catalytically by promoting the N-terminal phosphorylation of β-cat.

Phospho–β-cat and components of the destruction complex localize to cell–cell contacts in a complex that is distinct from cadherins

To further characterize this mechanism, we sought to determine the subcellular localization and fractionation characteristics of these phospho forms of β-cat. Of interest, β-cat phosphorylated at either Thr41 and Ser45 (P41/45) or Ser33, Ser37, and Thr41 (P33/37/41) can localize to cadherin-containing cell contacts in cultured cells (Fig. 2, A, B, H, and I) as well as in situ at adherens junctions in a normal epithelial tissue that exhibits Wnt/
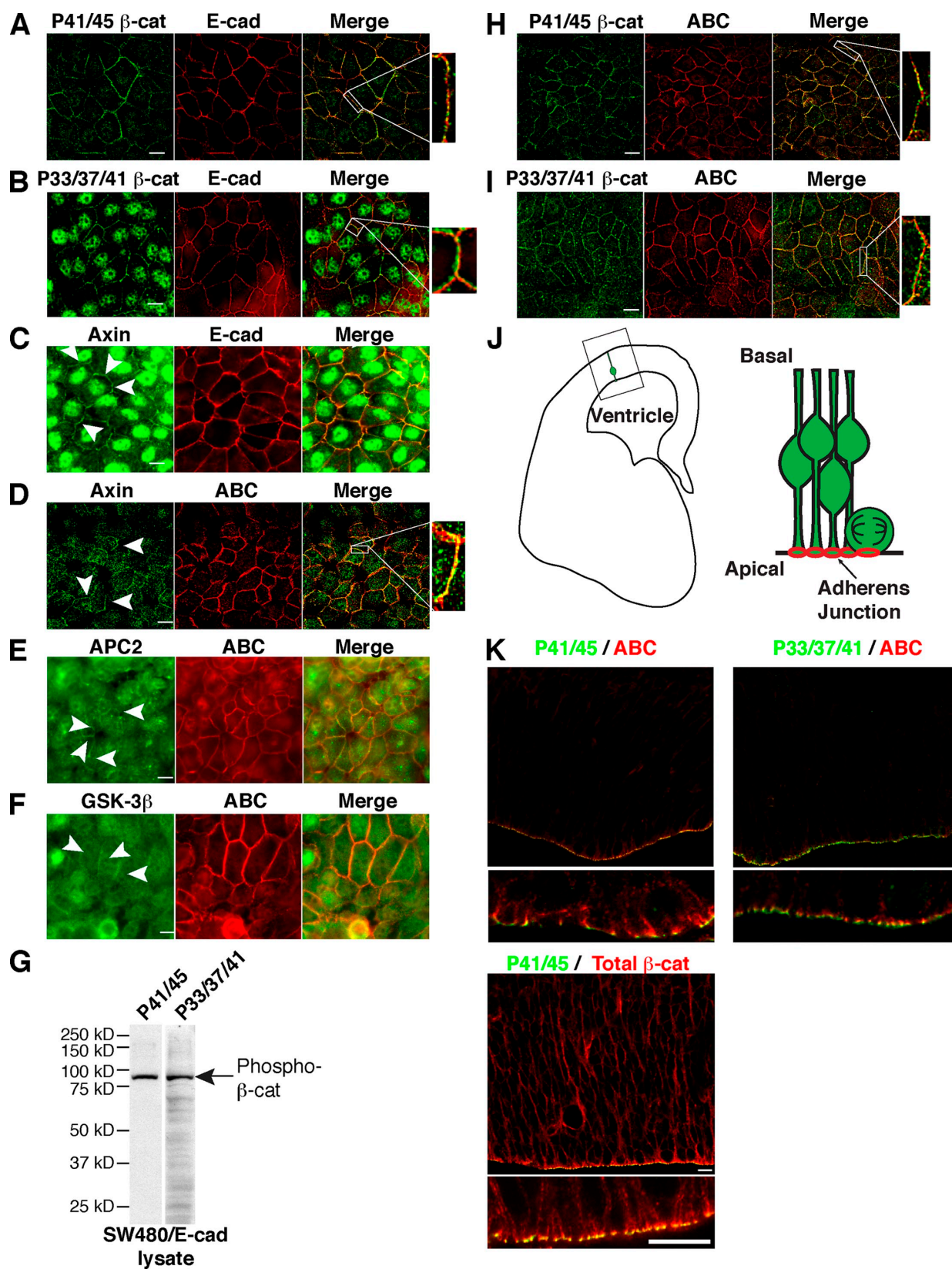
Figure 2. **Phospho–β-cat and components of the destruction complex localize to cell contacts.** (A–D, H, and I) Antibodies to P41/45 and P33/37/41 β-cat (A and B) and axin (C) stain cell contacts but fail to completely colocalize with E-cad (merge, white boxes) or ABC (D, H, and I). (E and F) Antibodies to APC2 (E) and GSK-3β (F) also reveal staining at cell contacts. Note that monolayers in E and F were saponin extracted before fixation to reveal contact localization. (C–F) Arrowheads indicate cell contact staining. (G) Immunoblot of SW480/E-cad lysate shows that the major band detected by P41/45 and P33/37/41 antibodies is 92 kD, the molecular mass of β-cat. (J) Brain schematic showing location of ventricular zone and orientation of neuroepithelial cells. (K) Immuno-fluorescence images of mouse ventricular zone show lack of P41/45 and P33/37/41 with ABC at adherens junctions. Bars, 10 μm.

β-cat signaling (Fig. 2, J and K; and Fig. S1 A; Woodhead et al., 2006). Because these phospho forms of β-cat are only partially colocalized with cadherin and ABC (Fig. 2 and Fig. S1 A), we asked whether components of the β-cat phosphodestruction complex also localize to cell contacts. Indeed, immunofluorescence analysis of E-cad–expressing SW480 cells reveals that axin, APC2, and GSK-3β can be detected at cell contacts (Fig. 2, C–F). Although diffuse cytoplasmic and nuclear localizations of these proteins are also evident, as previously described (Henderson, 2000; Cong and Varmus, 2004), these data agree with earlier studies demonstrating APC2 and axin localization to cell contacts in *Drosophila melanogaster* and *Xenopus laevis*, respectively (Fagotto et al., 1999; McCartney et al., 1999; Yu et al., 1999; Jarrett et al., 2001).

Given that phospho–β-cat and axin do not fully colocalize with E-cad at cell contacts (Fig. 2, A–C), we examined whether these proteins participate in different molecular complexes. A membrane fraction was isolated from E-cad–expressing SW480 cells (Fig. 3 A; Gottardi and Gumbiner, 2004a) and subjected to sucrose density gradient centrifugation (Fig. 3 B). Using this method, we observe that E-cad floats to the top of the gradient in a light sucrose fraction as expected for a transmembrane protein (Fig. 3 C, ii, lanes 6 and 7), whereas total β-cat partitions equally between this E-cad fraction and more dense fractions (Fig. 3 C, iii, lanes 1–3). Remarkably, these two peak fractions of β-cat can be distinguished by their N-terminal phosphorylation status, such that dense fractions contain β-cat phosphorylated at 33/37/41 and 41/45 (Fig. 3 C, v and vi), whereas ABC predominantly floats with E-cad in light fractions (Fig. 3 C, iv, lanes 6 and 7). Although some ABC is observed in the denser fractions, this could result from a lag in coupling the priming phosphorylation at Ser45 to phosphorylation at GSK-3β sites 41, 37, and 33 (Fig. 3 C, iv, lanes 2–5). Most of the ABC at cell contacts fails to colocalize with the phospho forms of β-cat (Fig. 2, H and I, merge, white box), suggesting that ABC is largely associated with the cadherin adhesive complex. Consistent with evidence that phosphorylation of β-cat occurs more efficiently in the presence of the axin complex (Dajani et al., 2003), axin, APC2, truncated APC, and GSK-3β cosediment with phospho–β-cat in the dense sucrose fractions (Fig. 3 C, vii–x, lanes 1–3). Together, these data suggest that the phospho–β-cat observed at cell contacts may be localized to the membrane through an association with the axin–phosphodestruction complex rather than binding to E-cad.

Given that cadherin expression was associated with a reduction in ABC and increase in phosphorylation at this epitope (Fig. 1), we assessed whether cadherin expression might alter the fractionation characteristics of the phospho–β-cat–axin complex. As expected for the parental SW480 cells, total membrane-associated β-cat and ABC are largely associated with dense fractions because of the low level of E-cad expression compared with SW480/E-cad cells (Fig. 3 D, ii and iii). However, axin, GSK-3β, APC2, and phospho–β-cat forms continued to cosediment in the dense sucrose fractions (Fig. 3 D, iv–vii, lanes 1 and 2; and not depicted). These data suggest that E-cad does not affect the sedimentation characteristics of the membrane-associated axin–phosphodestruction complex.

It is formally possible that the sedimentation of phospho–β-cat and components of the destruction complex to dense fractions could be caused by its large size rather than bona fide membrane association. Therefore, we sought to demonstrate that these components are membrane glycoprotein associated using the lectin Con A. As expected, we find that restoring cadherin expression in SW480 cells increases the amount of E-cad, total β-cat and ABC that can be affinity precipitated with Con A beads (Fig. 3 F). Although axin, GSK-3β, and APC2 (Fig. 3 F and not depicted) can be precipitated by Con A, restoring cadherin expression did not increase the abundance of these components in the glycoprotein fraction. The activity of GSK-3β was also not altered, at least with regard to the inhibitory phosphorylation at Ser9. However, cadherin expression did increase the amount of the phospho–β-cat recruited to a glycoprotein fraction (Fig. 3 F). Altogether, these data suggest that cadherins may be able to reduce the signaling form of β-cat indirectly by promoting β-cat recruitment to and/or flux through the phosphodestruction complex.

Cell–cell adhesion limits accumulation and activity of the signaling form of β-cat

To explore this mechanism further, we assessed whether changes in cadherin-based adhesion could impact the signaling form of β-cat in normal human epidermal keratinocytes (NHEKs), which are highly amenable to the Ca^{2+} switch approach to control the formation or dissolution of cadherin-based adhesions (Watt et al., 1984). To determine whether cell adhesion could impact the accumulation of cytosolic β-cat during a Wnt-like signal, NHEKs were stimulated with the Wnt mimic LiCl in the presence of low or normal Ca^{2+}, and β-cat was affinity precipitated with GST–inhibitor of catenin and TCF (ICAT). ICAT is a small protein that binds to β-cat in the same region as cadherins and can be used to isolate a cadherin-free cytosolic pool of β-cat (Gottardi and Gumbiner, 2004b). We observe that loss of cadherin-based adhesion (low Ca^{2+}) results in enhanced accumulation of cytosolic β-cat (Fig. 4 A) as well as the hypophosphorylated form (Fig. 4 B, ABC). Importantly, this phenomenon occurs in the absence of changes in cadherin protein levels (Fig. 4, A and B), or the amount of β-cat association with the cadherin (Fig. 4 C). The increase in β-cat correlates with enhanced transcriptional activation of the β-cat target gene *Axin2* (Fig. 4 D). Cell adhesion can also limit a bona fide Wnt signal, as Wnt3a-activated alveolar epithelial cells show a density-dependent reduction in *Axin2* expression (Fig. 4 F). These data indicate that cell–cell adhesion can attenuate β-cat transcriptional activity by limiting accumulation of the signaling form of β-cat.

Cell–cell adhesion enhances β-cat turnover

Our observation that Ca^{2+}-dependent adhesion limits the accumulation of cytosolic β-cat independent of changes in the cadherin complex suggests that β-cat turnover may be enhanced by adhesion. To test this directly, we measured the turnover of cytosolic β-cat in the presence or absence of robust cell contacts in MDCK cells. The phospho forms of β-cat localize to cell–cell contacts in these cells and exhibit fractionation characteristics similar to E-cad–expressing SW480
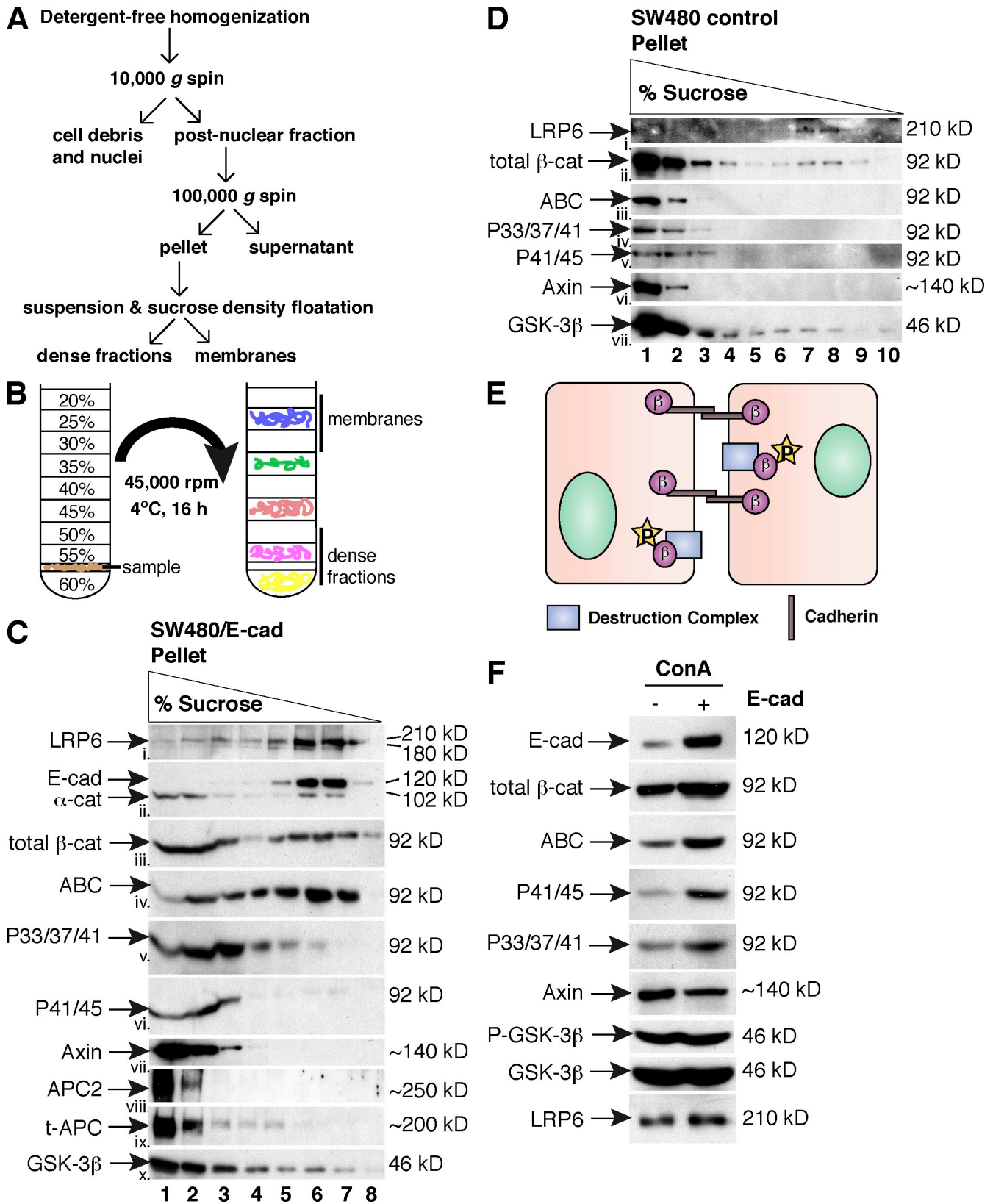
Figure 3. **Phospho–β-cat and components of the destruction complex do not cofractionate with cadherins.** (A and B) Outline of crude membrane fractionation (A) and sucrose density equilibrium centrifugation (B) methods. (C and D) Immunoblots from sucrose fractionation of E-cad–expressing (C) and control SW480 cells (D). α-cat, α-catenin; t-APC, truncated APC. (E) Schematic of findings from C. β, β-cat; P, phosphate group. (F) Con A fraction from control and SW480/E-cad cells immunoblotted with the antibodies shown. The pull-down efficiency of E-cad is 90% of input; the pull-down efficiency of phospho–β-cat, axin, and GSK-3β is 5%. P–GSK-3β, phospho–GSK-3β.
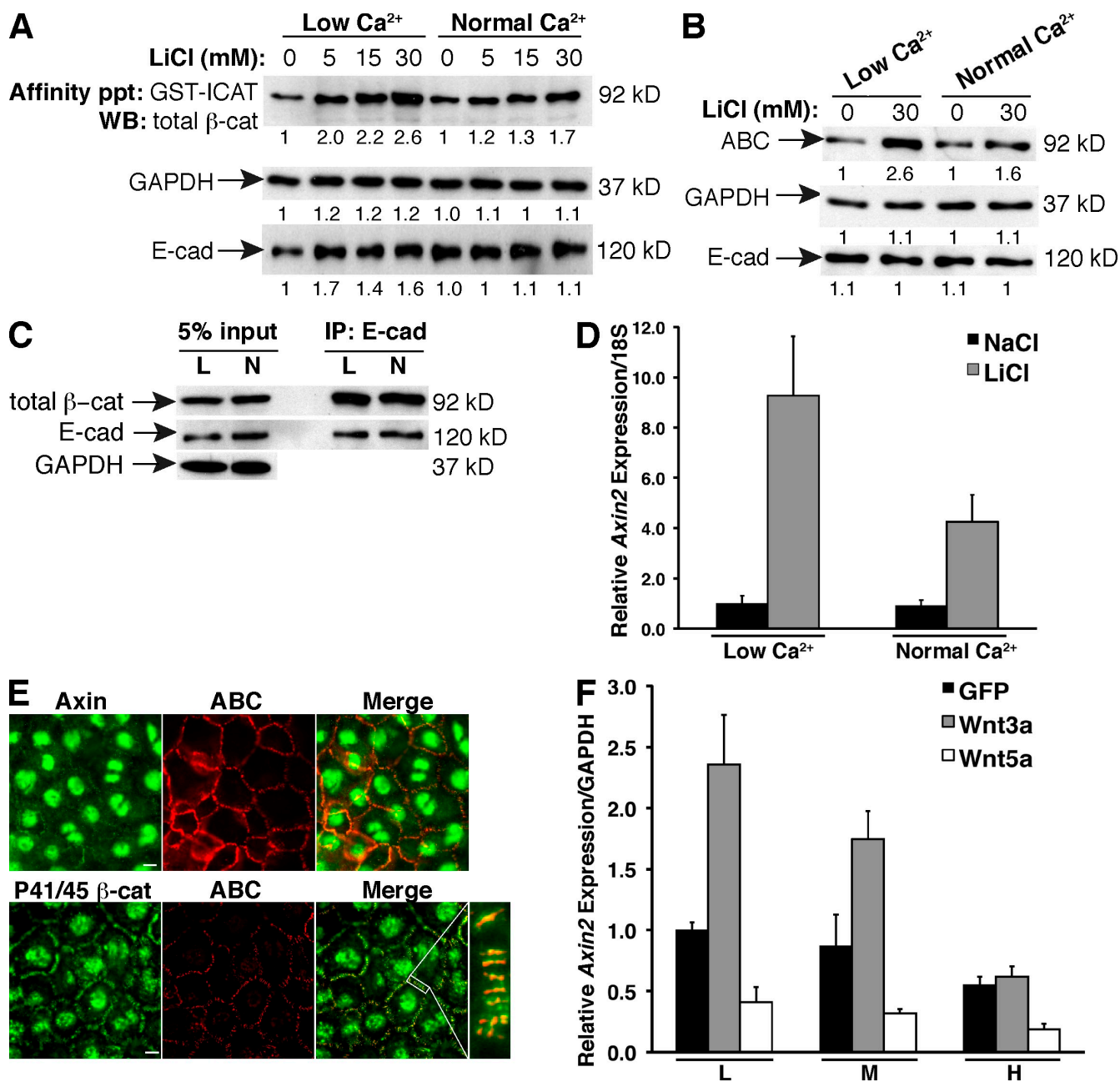
Figure 4. **Adhesion limits the abundance and activity of the β-cat signaling pool.** (A) Lysates from NHEKs treated with different doses of LiCl in low or normal Ca²⁺ were affinity precipitated (affinity ppt) with GST-ICAT to isolate cytosolic β-cat. GAPDH and E-cad loading controls were taken from inputs. WB, Western blot. (B) Lysates from NHEKs treated with LiCl or NaCl (0) in low or normal Ca²⁺ were immunoblotted with the antibodies shown. (A and B) The numbers below each lane reflect normalized densitometry values. (C) Lysates from low (L) and normal (N) Ca²⁺–treated cells immunoprecipitated for E-cad and blotted for β-cat. (D) *Axin2* expression by qPCR in LiCl-activated NHEKs in low or normal Ca²⁺. Fold change was calculated by normalizing to the low Ca²⁺/NaCl sample. (E) Axin and P41/45 β-cat localize to cell contacts in NHEKs. Cell contact staining of P41/45 is absent in β-cat⁻/⁻ mouse keratinocytes, indicating that the staining is specific (Fig. S1 B). The white box shows the area of cell contact shown at higher magnification to the right. (F) *Axin2* expression by qPCR in GFP-, Wnt3a-GFP–, or Wnt5a-GFP–infected lung cells cultured at low (L), medium (M), or high (H) density. (D and F) Error bars represent standard deviation of triplicate samples. Bars, 10 μm.

cells (Fig. S2, A and B). As with NHEKs, treating MDCK cells with LiCl generated cytosolic β-cat, and this pool of β-cat was followed by affinity precipitation with GST-ICAT (Fig. S3 A) using the cycloheximide (CHX) chase method. Compared with low Ca²⁺ conditions, cytosolic β-cat disappears more rapidly in the presence of normal Ca²⁺ (Fig. S3 B). This difference in turnover does not appear to be caused by the low concentrations of Ca²⁺ itself because cells plated at

subconfluency possess more cytosolic β-cat than confluent cells and exhibit slower turnover rates (Fig. 5 A). Critically, cadherin protein levels and the integrity of the cadherin–catenin complex are unchanged by density (Fig. 5, A and B) or low Ca²⁺ conditions (Fig. S3 C), as previously described (McCrea and Gumbiner, 1991). Ca²⁺-dependent adhesion also limits Wnt3a-dependent β-cat accumulation (Fig. S3 D), indicating that the observed effect is not LiCl specific. Altogether,
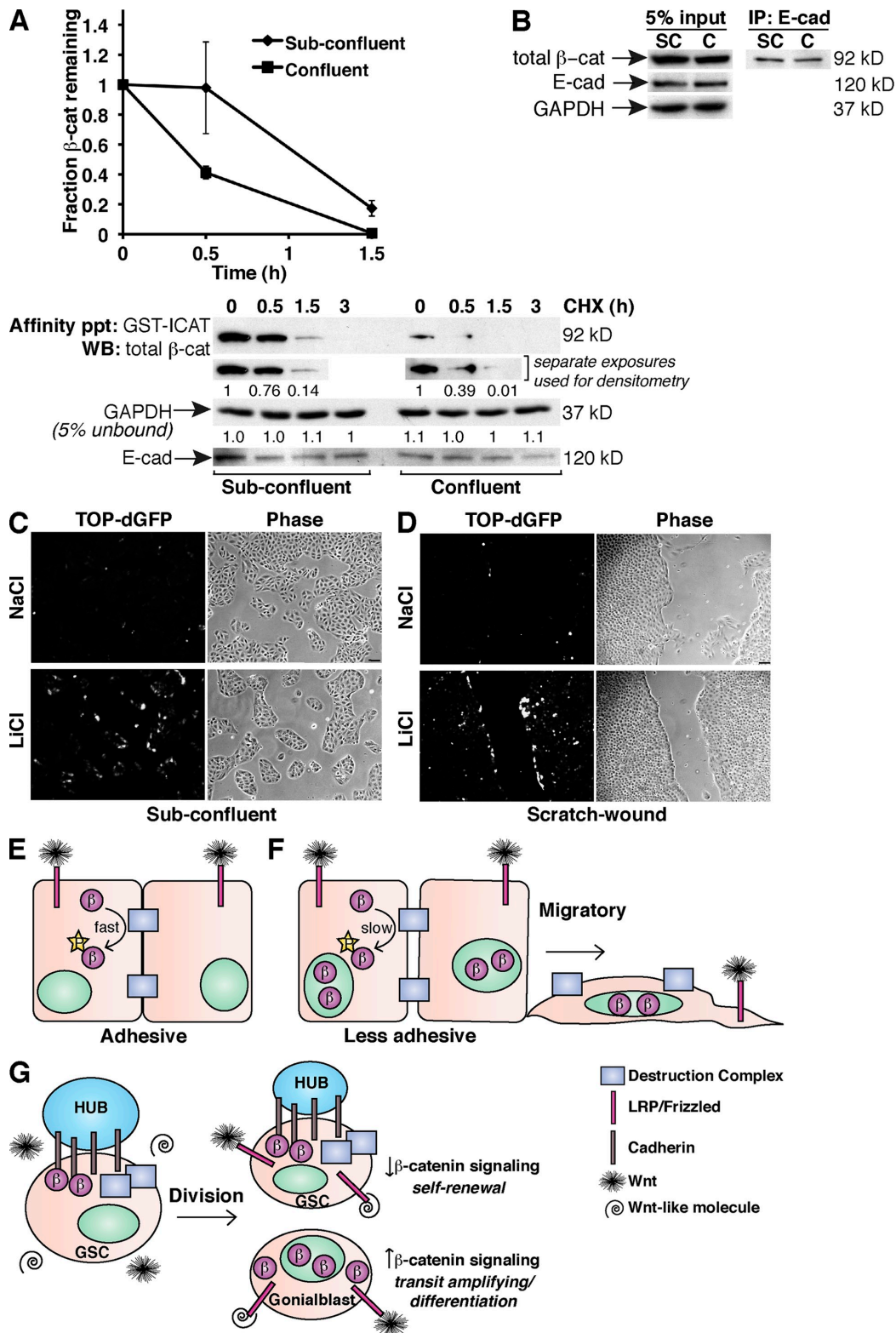
Figure 5. **Density-dependent turnover of cytosolic β-cat.** (A) Turnover of cytosolic (GST-ICAT bound) β-cat by CHX chase method from LiCl-treated subconfluent and confluent MDCK cells. Densitometry values were normalized to the t_0 value and plotted as shown. The plot represents the mean of two independent experiments; a set of representative immunoblots is shown. Error bars represent standard deviation of duplicate experiments. The numbers below each lane reflect normalized densitometry values. Affinity ppt, affinity precipitated; WB, Western blot. (B) Lysates from subconfluent (SC) and confluent (C) cells immunoprecipitated for E-cad and blotted for β-cat. (C and D) MDCK cells stably expressing TOP-dGFP show enhanced β-cat signaling in cells along a colony edge (C) and a scratch wound (D). (E) Cadherins promote the phosphorylation and turnover of β-cat in adhesive cells. (F) Less adhesive cells (e.g., migrations during wound healing) are sensitized to Wnt signals. (G) Adhesion-based modulation of Wnt signaling may be important in stem cell maintenance and differentiation. β, β-cat; GSC, germline stem cell; LRP, low density lipoprotein receptor–related protein; P, phosphate group. Bars, 30 µm.

these data suggest that cadherin-based adhesion may limit the extent and/or duration of Wnt/β-cat signals by enhancing the activity of a junction-localized phosphodestruction complex (Fig. 5 E). According to our model, when less adherent cells receive a Wnt signal such as during migrations that accompany wound healing, the ability of cadherins to activate the junction-localized degradation complex is somehow reduced, allowing the signaling pool of β-cat to persist (Fig. 5 F). Indeed, an MDCK clone that stably expresses a TCF optimal promoter (TOP)–destabilized GFP (dGFP; Dorsky et al., 2002) shows enhanced reporter activation in cells along the colony edge (Fig. 5 C) or scratch wounds (Fig. 5 D).

An appeal of this model is that it speaks to the long-standing notion that reductions in cell–cell adhesion may release β-cat for cell signaling. Although our data do not support a model in which β-cat dissociates from the cadherin, we do show that there is a membrane-localized form of phospho–β-cat that is not cadherin associated, raising the possibility that this β-cat may be freed from the membrane as a result of changes in intercellular adhesion. How the phosphodestruction complex is localized to cell contacts and how cadherins promote β-cat N-terminal phosphorylation within this complex are not understood.

It is becoming increasingly clear that a wide variety of molecular components can affect β-cat signaling, although a simple framework for explaining these effects has not emerged. For example, a *Drosophila* genetic screen for enhancers of β-cat signaling revealed that loss of proteins necessary for the establishment and maintenance of polarity such as the Fat cadherin, Stardust, and Discs large could enhance β-cat signaling (Greaves et al., 1999). More recently, components required for primary cilium structure/function and machineries that control planar cell polarity and convergence/extension movements can antagonize β-cat signaling at the level of Disheveled (Schwarz-Romond et al., 2002; Corbit et al., 2008). Although precise mechanisms are lacking, it is likely that many of these components ultimately affect the rate at which β-cat is consumed by the phosphodestruction complex. Because cadherin-based adhesion is a necessary prerequisite for polarity establishment, cilium formation, and planar cell polarity signaling, it may be difficult to tease out whether cadherins promote the activity of the phosphodestruction complex directly or through these other various inputs.

A model of adhesion-based modulation of Wnt signaling may also be relevant to asymmetric cell divisions that result in cells with distinct differentiative capacities, as seen in the *Drosophila* testes where a contact region between the germline stem cell and a cluster of somatic cells called the Hub is enriched with cadherins and APC2 (Yamashita et al., 2003). Specifically, we propose that cadherin-initiated inheritance and/or activation of a junction-localized β-cat phosphodestruction complex may generate daughter cells with different levels of β-cat signaling leading to distinct cellular outcomes (Fig. 5 G), suggesting an evolutionarily conserved mechanism relevant to development and stem cell biology.

Materials and methods

Cell culture and antibodies

SW480 and MDCK cells were obtained from American Type Culture Collection. E-cad–expressing SW480 cells were originally described in Gottardi et al. (2001). Both cell types were maintained in DME containing 10%. MDCK cells were transfected using Lipofectamine 2000 (Invitrogen), and colonies were selected in 0.8 mg/ml G418. Ca²⁺-free and 1.8 mM CaCl₂ DME were obtained from Invitrogen. The Ca²⁺-free media was adjusted to 5 µM Ca²⁺ with CaCl₂ (Sigma-Aldrich) to generate low Ca²⁺ media. NHEKs were isolated from human foreskin as previously described (Halbert et al., 1992). Cells were propagated in medium 154 supplemented with human keratinocyte growth supplement, 1,000× gentamycin/amphotericin B solution (Invitrogen), and 0.03 or 1.2 mM CaCl₂. Alveolar epithelial type 2 (AT2) cells were isolated from pathogen-free 200–225-g male Sprague-Dawley rats by the Pulmonary Core Facility at Northwestern University as previously described (Dobbs et al., 1986). In brief, lungs were perfused via the pulmonary artery, lavaged, and digested with 4 U/ml elastase (Worthington Biochemicals) for 20 min at 37°C. Tissue was minced and filtered through sterile gauze followed by 150- and 15-µm nylon mesh (Sefar), and the crude cell suspension was purified by differential adherence of non-AT2 cells to rat IgG–coated dishes (Sigma-Aldrich). AT2 viability is typically >93%, as determined by exclusion of Trypan blue stain. Purity is >90% by staining for lamellar bodies with Papanicolaou stain. AT2 cells are cultured in DME with 4.5 g/l glucose, L-glutamine, and Na pyruvate (Mediatech) plus 10% FBS (Hyclone) and penicillin/streptomycin (Mediatech). Wild-type and β-cat–null mouse keratinocytes were provided by E. Müller (University of Bern, Bern, Switzerland). Antibodies used were total β-cat, α-catenin, and neuronal cadherin (BD); ABC (clone 8E7; Millipore); axin (provided by R. Nusse, Stanford University, Stanford, CA); APC (Ab-1; EMD); APC2 (provided by S. Byers, Georgetown University, Washington, DC); P33/37/41, P41/45, GSK-3β, Ser9 phospho–GSK-3β, and LRP6 (Cell Signaling Technology); glyceraldehyde 3-phosphate dehydrogenase (GAPDH; Santa Cruz Biotechnology, Inc.); E-cad (HECD-1; Invitrogen); anti–dog E-cad (provided by B. Gumbiner, University of Virginia, Charlottesville, VA); and Alexa Fluor 488–, 555–, or 568–conjugated goat IgGs (Invitrogen).

Immunofluorescence

Cells were fixed in methanol or extracted with 0.05% saponin before fixation in 3% paraformaldehyde and processed using standard procedures. Coverslips were mounted with Aqua Poly/Mount (Polysciences). Images were captured with a microscope (Axioplan 2; Carl Zeiss, Inc.) equipped with a 63× Plan-Neofluar NA 1.25 objective, a camera (AxioCam HRm; Carl Zeiss, Inc.), and AxioVision4.6 software (Carl Zeiss, Inc.) and deconvolved using the inverse filtering method or with a laser-scanning confocal microscope (LSM 510; Carl Zeiss, Inc.) with a 63× Plan-Apochromat NA 1.4 objective and LSM 510 software (Carl Zeiss, Inc.). C57BL/6 and Swiss-Webster mice (*Mus musculus*) were treated according to protocols reviewed and approved by the Institutional Animal Care and Use Committee of Northwestern University. Immunofluorescence of embryonic day 15 brain cryosections was performed as previously described (Woodhead et al., 2006). Fixed tissues were mounted with a solution of 50% glycerol/50% PBS, and images (1-µm single optical slices) were captured using the LSM 510 microscope with a 40× Plan-Neofluar NA 1.3 or 100× Plan-Apochromat NA 1.4 objective. All immunofluorescent images were captured at room temperature and further processed using Photoshop CS3 (Adobe).

Sucrose equilibrium density gradient centrifugation

Detergent-free membrane fractions were prepared according to Gottardi et al. (2001) and resuspended in a 60% sucrose solution (20 mM Tris, pH 8.0, 100 mM NaCl, and 5 mM EDTA) as previously described (Reinacher-Schick and Gumbiner, 2001). Samples were applied on top of 0.5 ml of a 60% sucrose solution cushion in a 13 × 51–mm ultra-clear centrifuge tube (Beckman Coulter). A step gradient of sucrose solutions varying by 5% (from 55 to 20%) was poured over the sample. Gradients were centrifuged in an SW55Ti rotor (Beckman Coulter) at 45,000 rpm for 16 h at 4°C. Approximately 0.5-ml fractions were collected, and TCA was precipitated before immunoblot analysis.

Ca²⁺ switch experiments

Keratinocytes were seeded at density in 0.07 mM Ca²⁺ media and switched to either low (0.03 mM) or normal (1.2 mM) Ca²⁺-containing media 18 h before analysis. For supplemental experiments, MDCKs were

seeded in normal Ca^{2+} media containing 1.8 mM $CaCl_2$ and switched to either low (5 µM) or normal Ca^{2+}-containing media as described previously (Nigam et al., 1992).

Real-time PCR

Total RNA from NHEKs was isolated using the Aurum Total RNA Mini kit (Bio-Rad Laboratories) and from day 3 AT2 cells using RNeasy Plus Mini kit (QIAGEN). cDNA was synthesized using the iScript cDNA Synthesis kit (Bio-Rad Laboratories). Real-time quantitative PCR (qPCR) was performed with iQ SYBR green Supermix (Bio-Rad Laboratories) on an iCycler MyiQ single color real-time PCR detection system (Bio-Rad Laboratories). Relative change in gene expression was calculated using the ΔΔCt method. Primers are as follows: human Axin2 forward (5′-ACAACAGCATTGTCTCCAAGCAGC-3′) and reverse (5′-GCGCCTGGTCAAACATGATGGAAT-3′), human 18S forward (5′-CGTTGATTAAGTCCCTGCCCTT-3′) and reverse (5′-TCAAGTTCGACC-GTCTTCTCAG-3′), rat Axin2 forward (5′-AGATTCAGGCGGTGATGGAG-GAAA-3′) and reverse (5′-ACGGTGGGTGAAAGTTTGCACTTC-3′), and rat GAPDH forward (5′-GGTGAAGGTCGGAGTCAACG-3′) and reverse (5′-GGATTCCATTGATGACAAGCTTC-3′).

Affinity precipitation and immunoblotting

Cells were lysed in buffer containing 50 mM Tris, pH 7.5, 5 mM EDTA, 150 mM NaCl, 5% glycerol, and 1% Triton X-100 with protease inhibitor cocktail (Roche) and 1 mM microcystin (EMD). For NHEK experiments, 400–425 µg of total protein was incubated with 10 µg GST-ICAT precoupled to a 50% suspension of glutathione-coupled Sepharose beads (GE Healthcare) for 2 h at 4°C. For MDCK experiments, ~250 µg of lysates was incubated with 10 µg GST-ICAT and 50 µl of a 50% suspension of glutathione-coupled Sepharose beads for 2 h at 4°C. Con A–Sepharose (Sigma-Aldrich) precipitation experiments were performed as previously described (Gottardi et al., 2001). Precipitated proteins were washed and subjected to SDS-PAGE and immunoblot analysis using standard procedures. Densitometry was performed using the CanoScan software (Canon) and analyzed using ImageJ (National Institutes of Health).

Protein turnover

MDCK cells were cultured to subconfluency or confluency and treated with 30 mM LiCl for 18 h. Cells were then rinsed in PBS, incubated with 25 µg/ml CHX (EMD) in DME for the times indicated, lysed, and affinity precipitated as described in the previous section. For supplemental experiments, MDCK cells were grown to density and treated with 30 mM LiCl in either low or normal Ca^{2+}-containing media for 18 h. Cells were incubated with CHX in either low or normal Ca^{2+}-containing media as indicated, and lysates were processed as described in the previous section.

Wnt experiments

AT2 cells were infected in suspension on day 0 with 20 plaque-forming units of GFP control, Wnt3α-GFP, or Wnt5α-GFP adenovirus (provided by T.C. He, University of Chicago, Chicago, IL). Media was changed on day 2, and cells were harvested on day 3. MDCK cells were infected with 10 plaque-forming units of GFP control or Wnt3α-GFP adenovirus. 30 h after infection, media was changed to either low or normal Ca^{2+}-containing media for 18 h.

Live cell imaging experiments with TOP-dGFP

Stable-expressing MDCK cells were plated to subconfluency and treated for 18 h with 30 mM NaCl or LiCl before imaging. Confluent monolayers were wounded with a plastic pipet tip, wounds healed for 24 h, and cells were treated with NaCl or LiCl for 18 h. Images were captured at room temperature on a microscope (Eclipse TE200; Nikon) with a 10× Plan-Fluor NA 0.30 objective (Nikon) and camera (SPOT Insight 3.2.0; Veeco Instruments), analyzed with MetaMorph 6.2 (MDS Analytical Technologies), and processed using Photoshop CS3.

Online supplemental material

Fig. S1 shows that phospho forms of β-cat localize to the apical junctional complex in murine brain ventricular zone sections and do not colocalize with ABC. Fig. S2 shows phospho–β-cat and ABC localization and fractionation in MDCK cells. Fig. S3 shows the effect of low versus normal Ca^{2+}-dependent adhesion on cytosolic β-cat turnover kinetics, cadherin–β-cat–binding interaction, and Wnt3α-mediated accumulation of cytosolic β-cat. Online supplemental material is available at http://www.jcb.org/cgi/content/full/jcb.200811108/DC1.

Note added in review. While this paper was under review, a recent publication showed that neuronal cadherin can interact with axin and LRP5 to negatively regulate Wnt/β-cat signaling in osteoblasts through an apparently similar mechanism (Hay et al. 2009. *Mol. Cell. Biol.* 29:953–964).

References

Cong, F., and H. Varmus. 2004. Nuclear-cytoplasmic shuttling of Axin regulates subcellular localization of beta-catenin. *Proc. Natl. Acad. Sci. USA*. 101:2882–2887.

Corbit, K.C., A.E. Shyer, W.E. Dowdle, J. Gaulden, V. Singla, M.H. Chen, P.T. Chuang, and J.F. Reiter. 2008. Kif3a constrains beta-catenin-dependent Wnt signalling through dual ciliary and non-ciliary mechanisms. *Nat. Cell Biol.* 10:70–76.

Cox, R.T., C. Kirkpatrick, and M. Peifer. 1996. Armadillo is required for adherens junction assembly, cell polarity, and morphogenesis during *Drosophila* embryogenesis. *J. Cell Biol.* 134:133–148.

Dajani, R., E. Fraser, S.M. Roe, M. Yeo, V.M. Good, V. Thompson, T.C. Dale, and L.H. Pearl. 2003. Structural basis for recruitment of glycogen synthase kinase 3beta to the axin-APC scaffold complex. *EMBO J.* 22:494–501.

Dobbs, L.G., R. Gonzalez, and M.C. Williams. 1986. An improved method for isolating type II cells in high yield and purity. *Am. Rev. Respir. Dis.* 134:141–145.

Dorsky, R.I., L.C. Sheldahl, and R.T. Moon. 2002. A transgenic Lef1/beta-catenin-dependent reporter is expressed in spatially restricted domains throughout zebrafish development. *Dev. Biol.* 241:229–237.

Fagotto, F., N. Funayama, U. Gluck, and B.M. Gumbiner. 1996. Binding to cadherins antagonizes the signaling activity of beta-catenin during axis formation in *Xenopus*. *J. Cell Biol.* 132:1105–1114.

Fagotto, F., E. Jho, L. Zeng, T. Kurth, T. Joos, C. Kaufmann, and F. Costantini. 1999. Domains of axin involved in protein-protein interactions, Wnt pathway inhibition, and intracellular localization. *J. Cell Biol.* 145:741–756.

Gottardi, C.J., and B.M. Gumbiner. 2004a. Distinct molecular forms of β-catenin are targeted to adhesive or transcriptional complexes. *J. Cell Biol.* 167:339–349.

Gottardi, C.J., and B.M. Gumbiner. 2004b. Role for ICAT in beta-catenin-dependent nuclear signaling and cadherin functions. *Am. J. Physiol. Cell Physiol.* 286:C747–C756.

Gottardi, C.J., E. Wong, and B.M. Gumbiner. 2001. E-cadherin suppresses cellular transformation by inhibiting β-catenin signaling in an adhesion-independent manner. *J. Cell Biol.* 153:1049–1060.

Greaves, S., B. Sanson, P. White, and J.P. Vincent. 1999. A screen for identifying genes interacting with armadillo, the *Drosophila* homolog of beta-catenin. *Genetics*. 153:1753–1766.

Guger, K.A., and B.M. Gumbiner. 2000. A mode of regulation of beta-catenin signaling activity in *Xenopus* embryos independent of its levels. *Dev. Biol.* 223:441–448.

Ha, N.C., T. Tonozuka, J.L. Stamos, H.J. Choi, and W.I. Weis. 2004. Mechanism of phosphorylation-dependent binding of APC to beta-catenin and its role in beta-catenin degradation. *Mol. Cell.* 15:511–521.

Halbert, C.L., G.W. Demers, and D.A. Galloway. 1992. The E6 and E7 genes of human papillomavirus type 6 have weak immortalizing activity in human epithelial cells. *J. Virol.* 66:2125–2134.

Hart, M., J.P. Concordet, I. Lassot, I. Albert, R. del los Santos, H. Durand, C. Perret, B. Rubinfeld, F. Margottin, R. Benarous, and P. Polakis. 1999. The F-box protein beta-TrCP associates with phosphorylated beta-catenin and regulates its activity in the cell. *Curr. Biol.* 9:207–210.

Heasman, J., A. Crawford, K. Goldstone, P. Garner-Hamrick, B. Gumbiner, P. McCrea, C. Kintner, C.Y. Noro, and C. Wylie. 1994. Overexpression of cadherins and underexpression of beta-catenin inhibit dorsal mesoderm induction in early *Xenopus* embryos. *Cell*. 79:791–803.

Henderson, B.R. 2000. Nuclear-cytoplasmic shuttling of APC regulates beta-catenin subcellular localization and turnover. *Nat. Cell Biol.* 2:653–660.

Jarrett, C.R., J. Blancato, T. Cao, D.S. Bressette, M. Cepeda, P.E. Young, C.R. King, and S.W. Byers. 2001. Human APC2 localization and allelic imbalance. *Cancer Res.* 61:7978–7984.

Klaus, A., and W. Birchmeier. 2008. Wnt signalling and its impact on development and cancer. *Nat. Rev. Cancer*. 8:387–398.

Liu, C., Y. Li, M. Semenov, C. Han, G.H. Baeg, Y. Tan, Z. Zhang, X. Lin, and X. He. 2002. Control of beta-catenin phosphorylation/degradation by a dual-kinase mechanism. *Cell*. 108:837–847.

McCartney, B.M., H.A. Dierick, C. Kirkpatrick, M.M. Moline, A. Baas, M. Peifer, and A. Bejsovec. 1999. *Drosophila* APC2 is a cytoskeletally-associated protein that regulates wingless signaling in the embryonic epidermis. *J. Cell Biol*. 146:1303–1318.

McCrea, P.D., and B.M. Gumbiner. 1991. Purification of a 92-kDa cytoplasmic protein tightly associated with the cell-cell adhesion molecule E-cadherin (uvomorulin). Characterization and extractability of the protein complex from the cell cytostructure. *J. Biol. Chem*. 266:4514–4520.

Nigam, S.K., E. Rodriguez-Boulan, and R.B. Silver. 1992. Changes in intracellular calcium during the development of epithelial polarity and junctions. *Proc. Natl. Acad. Sci. USA*. 89:6162–6166.

Polakis, P. 2000. Wnt signaling and cancer. *Genes Dev*. 14:1837–1851.

Reinacher-Schick, A., and B.M. Gumbiner. 2001. Apical membrane localization of the adenomatous polyposis coli tumor suppressor protein and subcellular distribution of the β-catenin destruction complex in polarized epithelial cells. *J. Cell Biol*. 152:491–502.

Schwarz-Romond, T., C. Asbrand, J. Bakkers, M. Kuhl, H.J. Schaeffer, J. Huelsken, J. Behrens, M. Hammerschmidt, and W. Birchmeier. 2002. The ankyrin repeat protein Diversin recruits Casein kinase Iepsilon to the beta-catenin degradation complex and acts in both canonical Wnt and Wnt/JNK signaling. *Genes Dev*. 16:2073–2084.

Staal, F.J., M. Noort Mv, G.J. Strous, and H.C. Clevers. 2002. Wnt signals are transmitted through N-terminally dephosphorylated beta-catenin. *EMBO Rep*. 3:63–68.

van Es, J.H., C. Kirkpatrick, M. van de Wetering, M. Molenaar, A. Miles, J. Kuipers, O. Destree, M. Peifer, and H. Clevers. 1999. Identification of APC2, a homologue of the adenomatous polyposis coli tumour suppressor. *Curr. Biol*. 9:105–108.

van Noort, M., J. Meeldijk, R. van der Zee, O. Destree, and H. Clevers. 2002. Wnt signaling controls the phosphorylation status of beta-catenin. *J. Biol. Chem*. 277:17901–17905.

Watt, F.M., D.L. Mattey, and D.R. Garrod. 1984. Calcium-induced reorganization of desmosomal components in cultured human keratinocytes. *J. Cell Biol*. 99:2211–2215.

Willert, K., and K.A. Jones. 2006. Wnt signaling: is the party in the nucleus? *Genes Dev*. 20:1394–1404.

Woodhead, G.J., C.A. Mutch, E.C. Olson, and A. Chenn. 2006. Cell-autonomous beta-catenin signaling regulates cortical precursor proliferation. *J. Neurosci*. 26:12620–12630.

Yamashita, Y.M., D.L. Jones, and M.T. Fuller. 2003. Orientation of asymmetric stem cell division by the APC tumor suppressor and centrosome. *Science*. 301:1547–1550.

Yu, X., and M. Bienz. 1999. Ubiquitous expression of a *Drosophila* adenomatous polyposis coli homolog and its localization in cortical actin caps. *Mech. Dev*. 84:69–73.

Yu, X., L. Waltzer, and M. Bienz. 1999. A new *Drosophila* APC homologue associated with adhesive zones of epithelial cells. *Nat. Cell Biol*. 1:144–151.